ON MULTI-LAYERED PIPE ANALYSES CONSIDERING INTERFACE BINDING CONDITIONS

Ludimar Lima de Aguiar, ludimar@petrobras.com.br
Petrobras, CENPES – Research and Development Center, Av. Horácio Macedo, 950 – Cidade Universitária – Ilha do Fundão, Rio de Janeiro - RJ, Brasil
Carlos Alberto Almeida, calmeida@puc-rio
PUC-Rio, Pontifical Catholic University of Rio de Janeiro, Department of Mechanical Engineering, Rua Marquês de São Vicente 225 – Gávea, 22453-900, Rio de Janeiro - RJ, Brasil

Abstract. *In this paper a finite element model representation of straight beams, with multilayer material cross-section, is considered for the analysis of risers under in plane loadings. The model approach is based on an overall and simplified representation of the complexity in a riser cross-section structure and considers a set of homogeneous beams bounded by thin adhesive layers placed between them. Timoshenko's beam kinematics is employed in the numerical representation of the beam axial, bending and torsional displacements, all varying according to quadratic lagrangian functions. At the interface, slip conditions are modeled using a binding layer assumed under constant shear state of stress, due to relative displacements between beam layers. Solutions for multilayered beams under various loading and boundary conditions are evaluated and compared to some analytical solutions, also presented in the paper.*

Keywords*: finite element model, Timoshenko's beam kinematics, multilayer material pipe, interlayer slip*

1. INTRODUCTION

Solutions for multi-layered beams have been proposed in the literature in both simplified closed form solution as well as more general numerical approaches. First analytical solutions on the subject are dated of the early 50's in a paper by Newmark et al.(1951), where a two-layered beam is considered using Euler-Bernoulli associated model, under linear assumptions for displacements, material constitutive law and constraints. More recently some other attempts for more general analytical solutions have been proposed. Girhammar and Gopu (1991,1993), Girhammar and Pan (2007) and Girhammar (2008) have presented first and second order analysis solutions with interlayer slip considered from an approximate to a more rigorous procedure, from specific to a generalized approximate second order analysis procedure, that allowed estimations for the magnitude of the deformations and the internal actions between layers. With the use of numerical tools, other models have been proposed to investigate the occurrence of partial shear interactions in beam-columns. Chen et al (2007) included the combined action of arbitrary transverse loading and constant axial force in a non-uniform slip stiffness model and Xu et al. (2007) extended the work to dynamic and buckling behavior of partial-interaction composite members including the influence of transverse shear deformations and cross-section rotary inertia. In a further work (Wu et al., 2007) these authors proposed an extension of their results by proposing an approximate simple expression of the beam-column fundamental frequency under axial loadings. In the same line, but using the finite element method approach, Jeong et al.(2005) developed a formulation that takes into account the partial interaction behavior of concrete-steel composite members, using finite elements in the interface idealization based on push-out test results of composite members. In a three-model study, Zona et al.(2011) compared the finite element formulations of an extended Euler-Bernoulli formulation and a Timoshenko's beam model to evaluate, for various loadings, the shear deformability of steel slab components, the collapse loadings, and the internal forces in each model. They show that displacement and stress results of a composed member are controlled by the interaction between bending and shear, i.e. short or long beams, in each case study. Using the same approach the behavior of a general multi-stacked composite beam with interlayer slip is treated in Sousa Jr. et al. (2010) where curvature locking difficulties are identified. It was concluded that the proposed model, that represents composed beams as an association of beams and interface elements, provides an efficient solution for the multilayered beam problem.

In this work the analysis of multilayered pipe-beams is numerically investigated, under Timoshenko's beam model assumptions, with axial, bending and torsional degrees-of-freedom, all interpolated along the element length using quadratic lagrangian functions. A novel representation in a single element model, including beams and interlayer deformation conditions, is approached considering the usual deformation energy of beams and constant through thickness shear state of stresses at each interlayer, for all loading conditions. As per the model numerical representation, interlayer materials have thicknesses much smaller than other cross-section dimensions. The formulation has been implemented and some solution results are presented to evaluate the accuracy of the model assumptions used in the approximate analysis procedure.

2. TWO-LAYER PIPE FORMULATION

2.1. Analytical Solution

In this section, the analytical solution for displacements in a two-layer pipe, under axial loading as shown in Fig. 1, is obtained. Two axial forces Fx_a and Fx_b acting at internal and external layers of the free end B, respectively, are considered with both layers restrained at A and bound by an adhesive material layer of small thickness h.

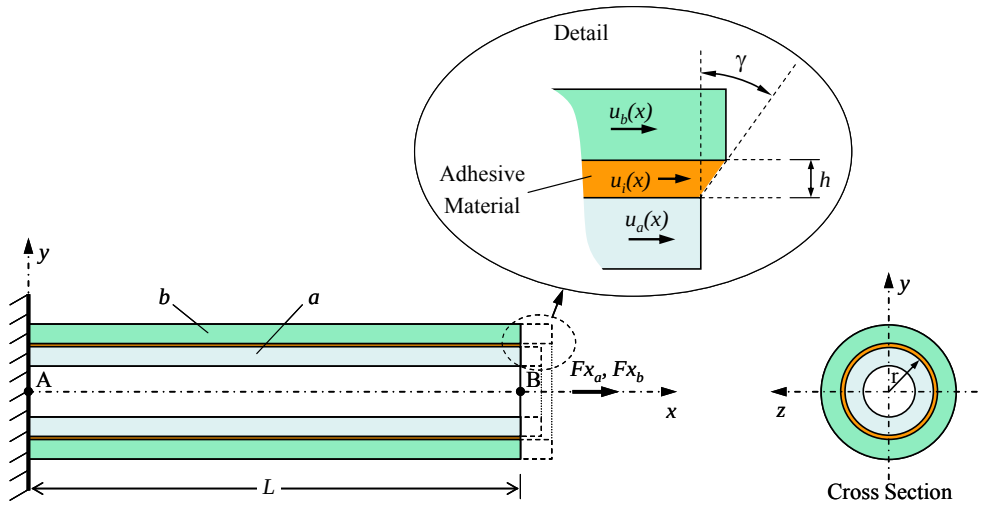

Figure 1. Axially loaded two-layer pipe bar.

From the detail presented in Fig. 1, the displacement field at the interface material is given by

$$u_i(x) = u_a(x) + \frac{u_b(x) - u_a(x)}{h}(y - r). \tag{1}$$

The interlayer thickness h is assumed small compared to the radius r, so that the shear strain in the adhesive material can be considered constant along thickness. Thus, shear strains (γ_i) and stresses (τ_i) at the interface are reduced to

$$\gamma_i = \frac{du_i}{dy} = \frac{u_b - u_a}{h} \quad \text{and} \quad \tau_i = G\gamma = \frac{G}{h}(u_b - u_a) \tag{2}$$

where G is the adhesive material shear modulus.

Considering the equilibrium conditions at both layers, the analytical solution for the displacement fields at layers a and b are obtained

$$u_a(x) = \frac{(C_1 + C_2 x)}{B} + \left(1 - \frac{E_b A_b}{2\pi r k}\frac{B}{A}\right)\left(C_3 e^{\frac{\sqrt{AB}}{A}x} + C_4 e^{-\frac{\sqrt{AB}}{A}x}\right) \tag{3}$$

$$u_b(x) = \frac{(C_1 + C_2 x)}{B} + C_3 e^{\frac{\sqrt{AB}}{A}x} + C_4 e^{-\frac{\sqrt{AB}}{A}x} \tag{4}$$

where: $A = \dfrac{E_a A_a E_b A_b}{2\pi r k}$ and $B = E_a A_a + E_b A_b$;

A_a, A_b, E_a and E_b are cross section areas and Young modulii for each material layer;

r is the radius of the interface;

$k = \dfrac{G}{h}$ is the interlayer material equivalent stiffness; and,

C_1, C_2, C_3 and C_4 are constants, obtained by imposing boundary conditions.

2.2. Finite Element Formulation

Solution for bending and torsional loadings cannot be obtained analytically. Thus, the numerical approach using Finite Elements is here employed. In this case, the formulation of the two-layer pipe beam element with interlayer slip is obtained under the following set of assumptions: small displacements, rotations and strains in both layers; in each layer the pipe follows Timoshenko's beam theory; both layers are continuously connected with no separation; and interaction between layers is considered at interlayer material of small thickness (h).

The two-layer pipe beam considered is presented in Fig. 2. Two different materials are employed at internal and external layers, which are marked with letters a and b, respectively. The beam is restrained to displacements and rotations at end A while at the free end B, axial, transverse, torsion and bending moment loads are applied to each layer, named Fx_a, Fx_b, T_a, T_b, Fy_a, Fy_b, M_a and M_b.

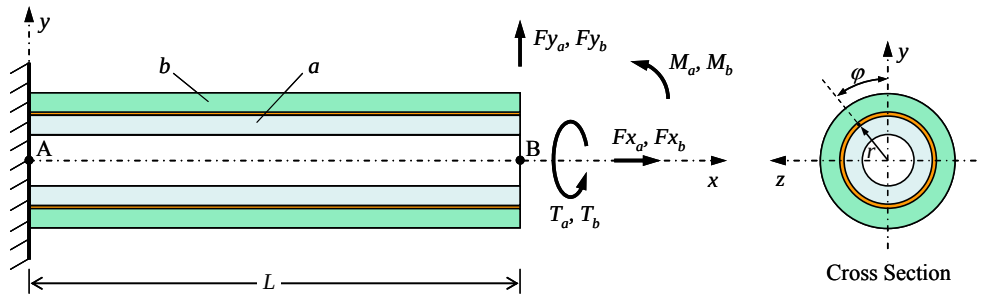

Figure 2. Two-layer pipe beam – undeformed configuration

Figure 3 presents the beam deformed shape, displacements and rotations of each layer all varying along the length.

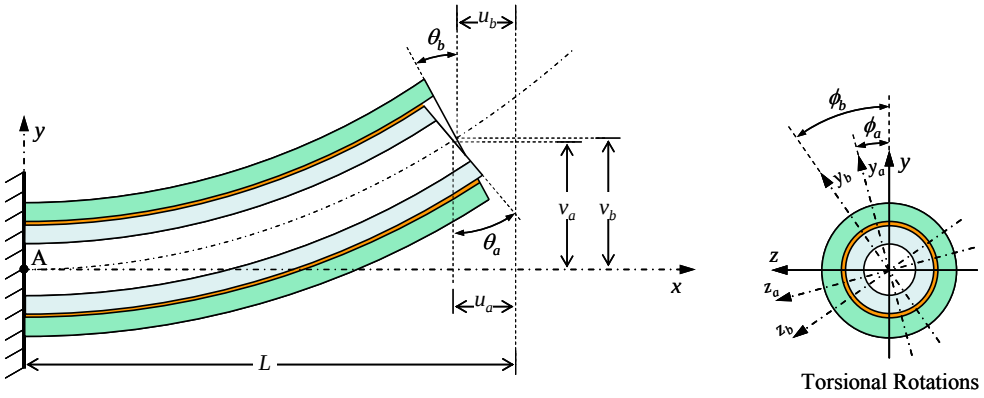

Figure 3. Two-layer pipe beam – deformed configuration

Following the Principle of Energy Conservation the equilibrium equations are obtained from the variation of the total potential energy (Π) of the beam, Bathe, K.J.(1996). In this case, this functional Π consists of three parts: axial and shear strain energies in each layer, shear strain energy in the interlayer material and external load work. The axial strain energy in both layers is given by

$$\pi_{\sigma_{xx}} = \underbrace{\frac{1}{2}\int_0^L E_a\left[A_a\left(\frac{du_a}{dx}\right)^2 + I_a\left(\frac{d\theta_a}{dx}\right)^2\right]dx}_{(\sigma_{xx})\,\text{internal layer}} + \underbrace{\frac{1}{2}\int_0^L E_b\left[A_b\left(\frac{du_b}{dx}\right)^2 + I_b\left(\frac{d\theta_b}{dx}\right)^2\right]dx}_{(\sigma_{xx})\,\text{external layer}} \tag{5}$$

where I_a, I_b are each layer cross section moments of inertia, respectively.

Assuming small displacements only, small slip between layers and no separation between layers, lateral displacements are the same for both layers, i.e. $v_a = v_b = v$. Thus, the shear strain energy in both layers is given by

$$\pi_\tau = \underbrace{\frac{1}{2}\int_0^L G_a\left[mA_a\left(\frac{dv}{dx}-\theta_a\right)^2 + J_a\left(\frac{d\phi_a}{dx}\right)^2\right]dx}_{(\tau)\text{ internal layer}} + \underbrace{\frac{1}{2}\int_0^L G_b\left[mA_b\left(\frac{dv}{dx}-\theta_b\right)^2 + J_b\left(\frac{d\phi_b}{dx}\right)^2\right]dx}_{(\tau)\text{ external layer}} \tag{6}$$

Where m is a geometric correction factor associated to transverse shear stress distribution in each layer cross section and J_a, J_b, G_a and G_b are the cross section polar moment of inertia and shear modulus for each layer, respectively.

The total external loading work is given by:

$$W = -F_{x_a}u_a(L) - F_{x_b}u_b(L) - F_y v(L) - M_a\theta_a(L) - M_b\theta_b(L) - T_a\phi_a(L) - T_b\phi_b(L) \tag{7}$$

Shear strains and stresses at the interface material, related to bending displacements are

$$\gamma_i(\varphi) = \frac{u_b - u_a - r(\theta_b-\theta_a)\cos\varphi}{h} \quad \text{and} \quad \tau_i(\varphi) = G\gamma_i(\varphi) = k(u_b - u_a - r(\theta_b-\theta_a)\cos\varphi) \tag{8}$$

and to torsion rotations are

$$\bar{\gamma}_i = \frac{r}{h}(\phi_b - \phi_a) \quad \text{and} \quad \bar{\tau}_i = G\bar{\gamma}_i = kr(\phi_b - \phi_a) \tag{9}$$

where φ is the angle position at the interface, as shown in Fig. 2.

Nonlinear slip between layers can be obtained with a suitable constitutive relation for the interlayer material where the equivalent stiffness $k(x,\varphi)$ may vary along the length and at the beam cross section. In this paper, all material models are assumed in the linear elastic range. Finally, the interlayer material strain energy

$$\pi_{\tau_i} = \frac{1}{2}\int_V \left(\tau_i\gamma_i + \bar{\tau}_i\bar{\gamma}_i\right)dV \tag{10}$$

results in

$$\pi_{\tau_i} = \frac{1}{2}\int_x\int_\varphi\int_r \frac{k}{h}\left[r(u_b - u_a - r(\theta_b-\theta_a)\cos\varphi)^2 + r^3(\phi_b-\phi_a)^2\right]drd\varphi dx \tag{11}$$

which is obtained substituting Eqs. (8) and (9) into Eq. (10). After integrating in radial and angular coordinates we have

$$\pi_{\tau_i} = \frac{1}{2}\int_0^L \pi kr\left[2(u_b-u_a)^2 + r^2(\theta_b-\theta_a)^2 + 2r^2(\phi_b-\phi_a)^2\right]dx\,. \tag{12}$$

By applying the principle of virtual work, Bathe,K.J.(1996),

$$\delta\Pi = \delta\pi_{\sigma_{xx}} + \delta\pi_\tau + \delta\pi_{\tau_i} + \delta W = 0\,, \tag{13}$$

where

$$\begin{aligned}
\delta\pi_{\sigma_{xx}} &= \int_0^L \left(E_aA_a\tfrac{du_a}{dx}\delta\tfrac{du_a}{dx} + E_aI_a\tfrac{d\theta_a}{dx}\delta\tfrac{d\theta_a}{dx} + E_bA_b\tfrac{du_b}{dx}\delta\tfrac{du_b}{dx} + E_bI_b\tfrac{d\theta_b}{dx}\delta\tfrac{d\theta_b}{dx}\right)dx \\
\delta\pi_\tau &= \int_0^L \left[mG_aA_a\left(\tfrac{dv}{dx}-\theta_a\right)\delta\left(\tfrac{dv}{dx}-\theta_a\right) + G_aJ_a\tfrac{d\phi_a}{dx}\delta\tfrac{d\phi_a}{dx}\right]dx \\
&\quad + \int_0^L \left[mG_bA_b\left(\tfrac{dv}{dx}-\theta_b\right)\delta\left(\tfrac{dv}{dx}-\theta_b\right) + G_bJ_b\tfrac{d\phi_b}{dx}\delta\tfrac{d\phi_b}{dx}\right]dx \\
\delta\pi_{\tau_i} &= \int_0^L \pi kr\left[2(u_b-u_a)\delta(u_b-u_a) + r^2(\theta_b-\theta_a)\delta(\theta_b-\theta_a) + 2r^2(\phi_b-\phi_a)\delta(\phi_b-\phi_a)\right]dx \\
\delta W &= -F_{x_a}\delta u_a(L) - F_{x_b}\delta u_b(L) - F_y\delta v(L) - M_a\delta\theta_a(L) - M_b\delta\theta_b(L) - T_a\delta\phi_a(L) - T_b\delta\phi_b(L)
\end{aligned} \tag{14}$$

Element displacement fields are then obtained, from nodal displacements, by using a suitable interpolation matrix $\mathbf{H}(\xi)$ in the form

$$\begin{bmatrix} u_a(\xi) \\ \theta_a(\xi) \\ \phi_a(\xi) \\ v(\xi) \\ u_b(\xi) \\ \theta_b(\xi) \\ \phi_b(\xi) \end{bmatrix} = \mathbf{H}(\xi)\hat{\mathbf{u}} \tag{15}$$

where ξ is the element local coordinate ($-\frac{l}{2} \le \xi \le \frac{l}{2}$);
l is the element length;
$\hat{\mathbf{u}}$ is the vector of nodal displacements of the element.

In this work a quadratic Lagrangian element is considered, as shown in Fig. 4, with the following interpolation functions $h(\xi)$

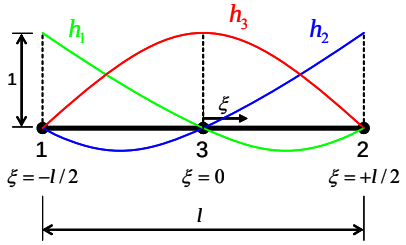

Figure 4. Longitudinal interpolation functions.

$$h_1(\xi) = \frac{\xi(2\xi - l)}{l^2},\ h_2(\xi) = \frac{\xi(2\xi + l)}{l^2} \text{ and } h_3(\xi) = -\frac{(2\xi + l)(2\xi - l)}{l^2} \tag{16}$$

These functions are defined in element domain $-\frac{l}{2} \le \xi \le \frac{l}{2}$ and, by taking displacements derivatives one obtains

$$\begin{bmatrix} \frac{du_a(\xi)}{d\xi} \\ \frac{d\theta_a(\xi)}{d\xi} \\ \frac{d\phi_a(\xi)}{d\xi} \\ \frac{dv(\xi)}{d\xi} \\ \frac{du_b(\xi)}{d\xi} \\ \frac{d\theta_b(\xi)}{d\xi} \\ \frac{d\phi_b(\xi)}{d\xi} \end{bmatrix} = \frac{d\mathbf{H}(\xi)}{d\xi}\hat{\mathbf{u}} = \mathbf{B}(\xi)\hat{\mathbf{u}} \text{ and, accordingly } \left[\delta \frac{\mathbf{d}}{\mathbf{d}\xi}\right] = \mathbf{B}(\xi)\delta\hat{\mathbf{u}} \tag{17}$$

Equation (13) results, for the complete element assemblage, in the following system of equations:

$$\mathbf{K}\hat{\mathbf{U}} = \mathbf{F} \tag{18}$$

where $\mathbf{K}$ is the global stiffness matrix resulting from each element stiffness matrix ($\mathbf{K}_e$);
$\hat{\mathbf{U}}$ is the nodal displacement vector for the whole structure;
$\mathbf{F}$ is the global external loading vector.

Thus, the element stiffness matrix associated to seven degrees-of-freedom per node is obtained as

$$\begin{aligned}\mathbf{K}_e &= \int_{-l/2}^{l/2}\left(E_a A_a \mathbf{B}_{u_a}^T \mathbf{B}_{u_a} + E_a I_a \mathbf{B}_{\theta_a}^T \mathbf{B}_{\theta_a} + E_b A_b \mathbf{B}_{u_b}^T \mathbf{B}_{u_b} + E_b I_b \mathbf{B}_{\theta_b}^T \mathbf{B}_{\theta_b}\right) d\xi \\ &+ \int_{-l/2}^{l/2} G_a \left[m A_a \left(\mathbf{B}_v^T - \mathbf{H}_{\theta_a}^T\right)\left(\mathbf{B}_v - \mathbf{H}_{\theta_a}\right) + J_a \mathbf{B}_{\phi_a}^T \mathbf{B}_{\phi_a} \right] d\xi \\ &+ \int_{-l/2}^{l/2} G_b \left[m A_b \left(\mathbf{B}_v^T - \mathbf{H}_{\theta_b}^T\right)\left(\mathbf{B}_v - \mathbf{H}_{\theta_b}\right) + J_b \mathbf{B}_{\phi_b}^T \mathbf{B}_{\phi_b} \right] d\xi \\ &+ \int_{-l/2}^{l/2} \pi k r \left[2\left(\mathbf{H}_{u_b}^T - \mathbf{H}_{u_a}^T\right)\left(\mathbf{H}_{u_b} - \mathbf{H}_{u_a}\right) + r^2 \left(\mathbf{H}_{\theta_b}^T - \mathbf{H}_{\theta_a}^T\right)\left(\mathbf{H}_{\theta_b} - \mathbf{H}_{\theta_a}\right) \right] d\xi \\ &+ \int_{-l/2}^{l/2} 2\pi k r^3 \left(\mathbf{H}_{\phi_b}^T - \mathbf{H}_{\phi_a}^T\right)\left(\mathbf{H}_{\phi_b} - \mathbf{H}_{\phi_a}\right) d\xi\end{aligned} \tag{19}$$

3. NUMERICAL EXAMPLES

In what follows numerical examples are set to demonstrate the efficiency of the new element in representing the two-layered pipe beam behavior, with interlayer slip. In the first example axial displacements are considered and the results compared to analytical solutions presented above. The next two examples show the responses of the beam under concentrated end bending and transverse loadings, respectively.

3.1. Pipe Beam Under Axial Loading

In this first example, a straight beam restrained in one end at layer *a* is loaded by an axial force F_b=*1000kN* applied at the free end of external layer *b*, as indicated in Fig. 6. The pipe's material and geometrical properties are presented in Tab. 1. These property values are set such that $E_aA_a = E_bA_b$, so that the interlayer shear stress distribution along the beam is symmetric. Solutions for various interlayer material stiffness '*k*' are presented.

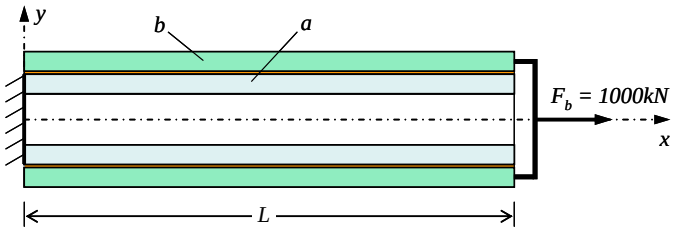

Figure 5. Pipe Beam Under Axial Loading

Table 1. Beam Property Considered in Analyses

Properties	Values
E_a *(KPa):*	1.557E+09
E_b *(KPa):*	2.070E+08
A_a *(m^2):*	0.003044
A_b *(m^2):*	0.022893
r (m):	0.163
L (m):	5.00

In this analysis a uniform twenty finite element mesh was employed. Figures 6, 7 and 8, show obtained numerical results for axial displacements and axial stresses at both materials and shear stresses at the interface material, respectively, as compared to analytical solutions. A very good agreement between numerical and analytical solutions is obtained.

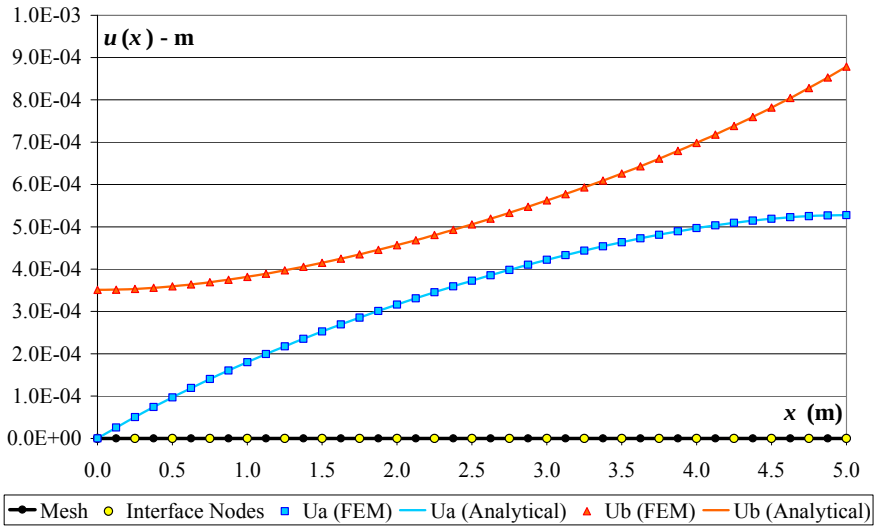

Figure 6: Axial displacements (k = *1000000*).

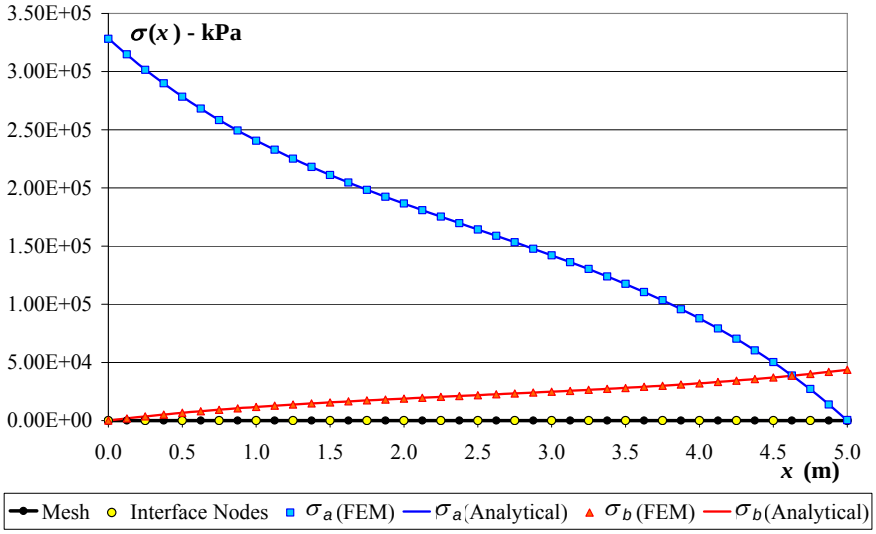

Figure 7: Axial stresses (k = *1000000*).

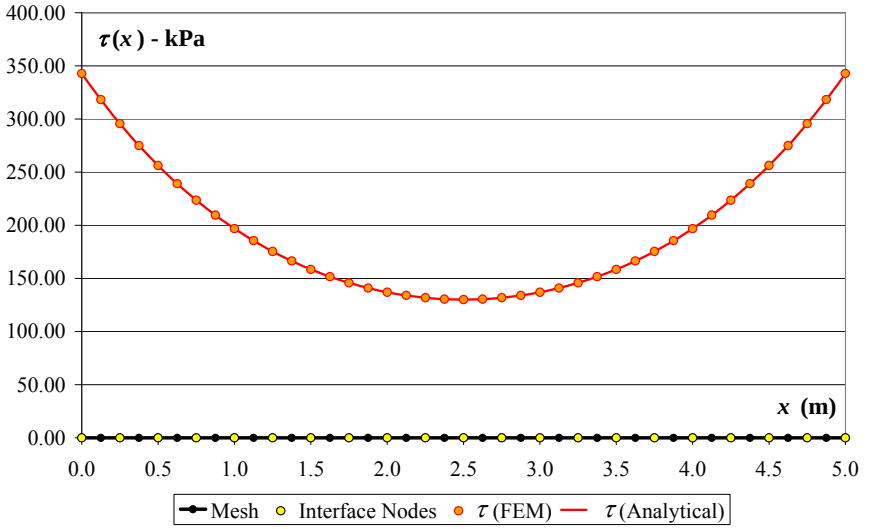

Figure 8: Shear stresses at the interface (k = *1000000*).

In Fig. 9 a sensitivity study solution for the interlayer material stiffness '*k*' is presented. The results show that for increasing values, interlayer shear stress distributions along the length of the pipe beam approach to zero while stress concentrations occur at beam both ends. These stress patterns suggest, as expected, layer delamination occurrence at these two end pipe positions, for practical values of the constant *k*.

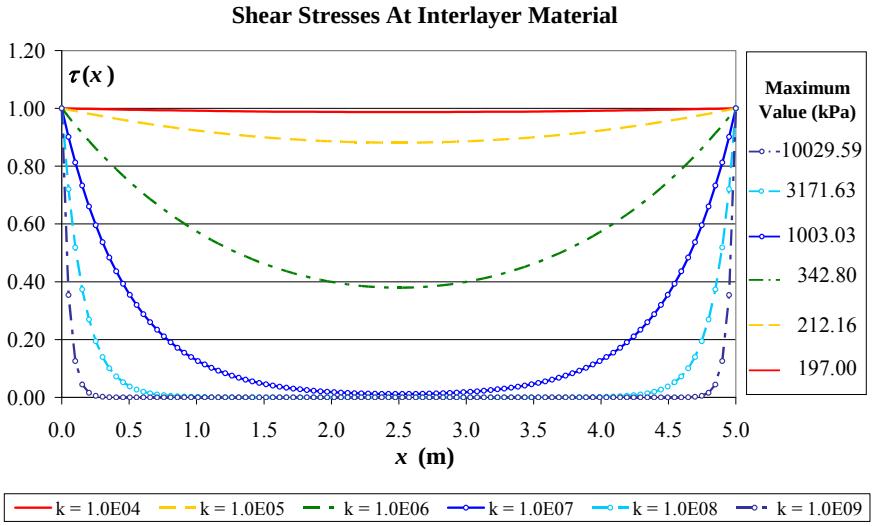

Figure 9: Sensitivity analysis results.

3.2. Cantilever Pipe Beam Under Constant Bending Moment

In this example a cantilever straight beam having the boundary conditions shown in Fig. 10 was considered for bending analysis. At clamped end only layer *a* is kept fixed while layer *b* is set free at both ends. A bending moment (M_a=*1000kNm*) is applied at the free end at layer *a*, as indicated in Fig. 10. Physical and geometric properties of the pipe beam are presented in Tab. 2 and a uniform thirty finite element mesh was used in this example.

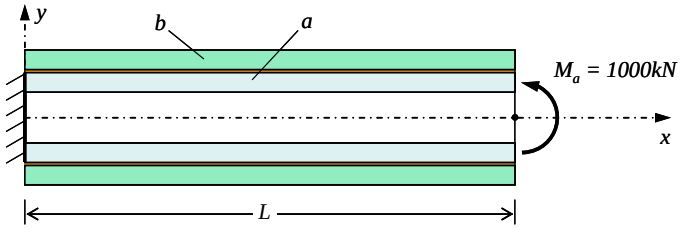

Figure 10. Boundary conditions – Pipe Beam Under Constant Bending Moment.

Table 2. Beam Properties for Bending Moment and Transverse Force Examples.

Properties	Values
E_a *(KPa):*	2.00E+08
E_b *(KPa):*	2.07E+08
A_a *(m^2):*	0.003044
A_b *(m^2):*	0.022893
r (m):	0.163
L (m):	5.00

Numerical results for *k=1000* are presented in Figs. 11, 12 and 13 for lateral displacements, rotations and bending moments, respectively. From these results all corresponding essential and natural boundary conditions are satisfied, expected slip conditions at both ends of the beam are well reproduced in Fig. 12 - by stress concentrations as in the previous example - and the condition of constant bending moment along the length of the pipe beam is provided in Fig. 13, taking into account the bending moment contribution at each beam due to shear stresses at the interface layer.

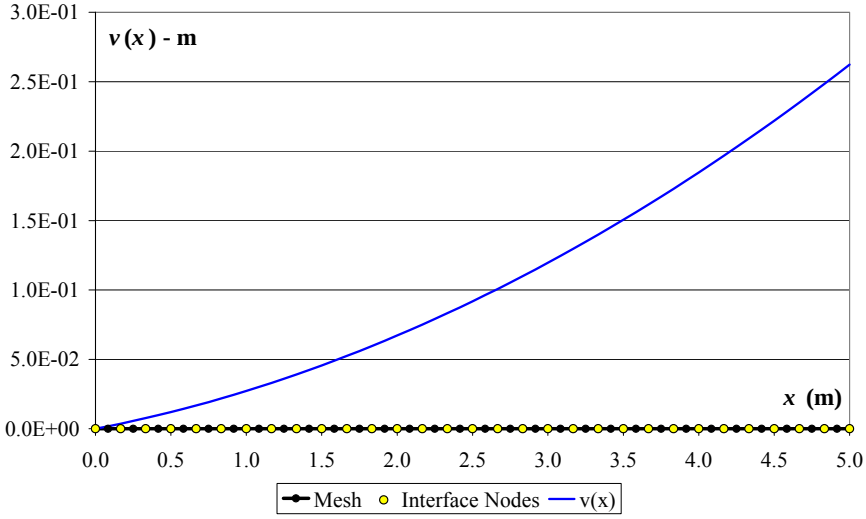

Figure 11: Lateral displacements (k = *1000*).

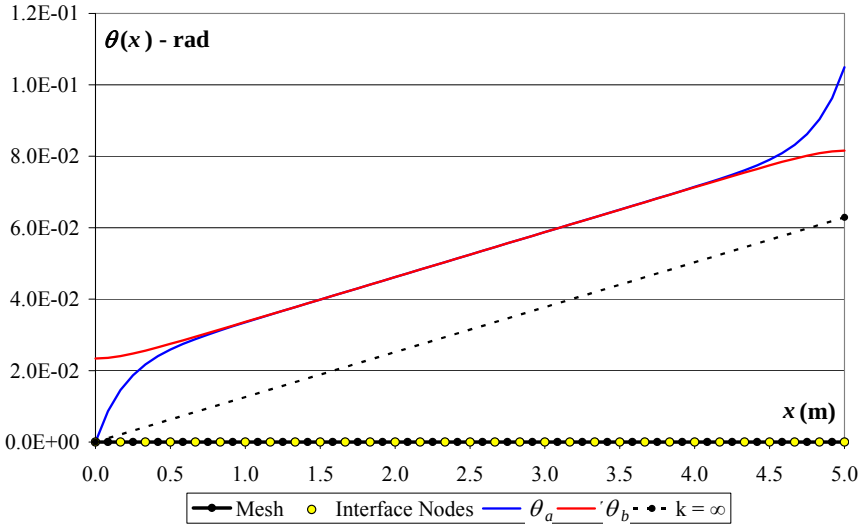

Figure 12: In plane rotations for each layer (k = *1000*).

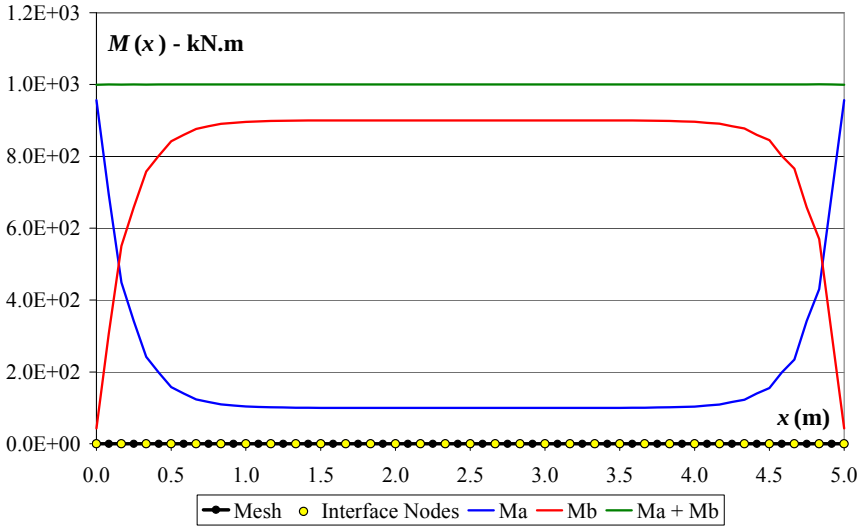

Figure 13: Bending moments (k = *1000*).

3.2. Pipe Beam Under Tip Transverse Loading

Figure 14 shows the cantilever beam considered with the outer layer constrained at the clamped side while a transverse force (*Fy=200kN*) applied at the free end. Geometrical and physical parameters are as in Table 2. Thirty equally spaced elements were used in this model analysis.

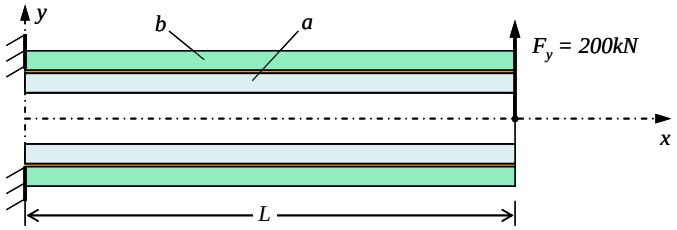

Figure 14. Boundary conditions – Pipe Beam Under Transverse Force Example.

Numerical results are presented in Figs. 15, 16, 17 and 18 for lateral displacements, in plane rotations, bending moments and axial stresses at each layer, respectively. From these results all corresponding essential and natural boundary conditions are numerically satisfied. Moment equilibrium at the beam cross-section along the element's length is also verified, as in shown in Fig. 17. The distribution shown is due to the shear stresses at the interface layer. Axial stress distributions presented in Fig. 18 are directly obtained from the results in Fig.17.

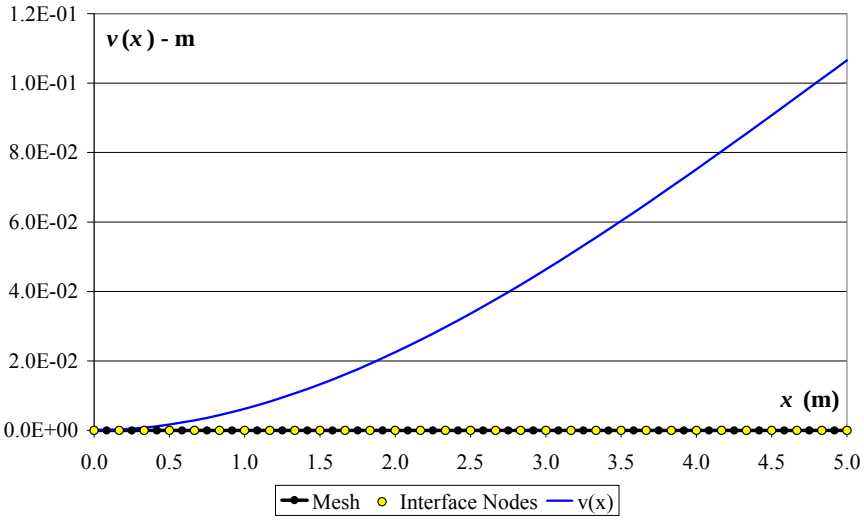

Figure 15: Lateral displacements (*k = 1000*).

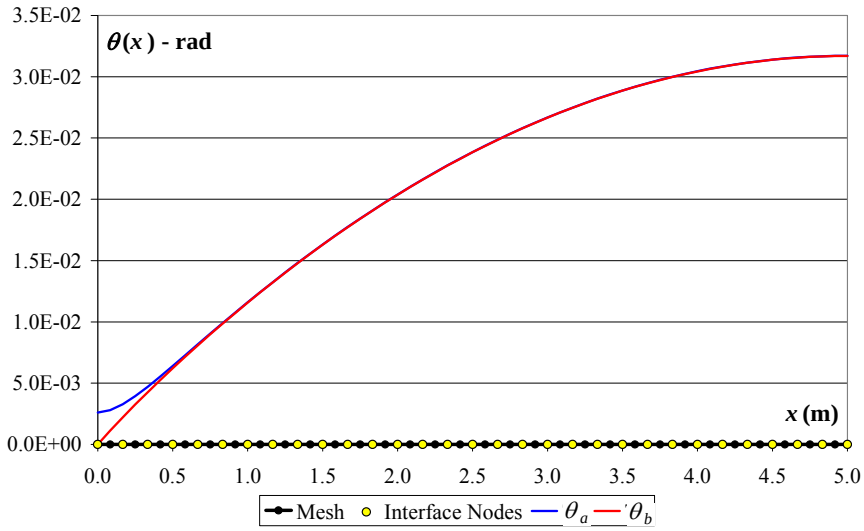

Figure 16: In plane rotations (*k = 1000*).

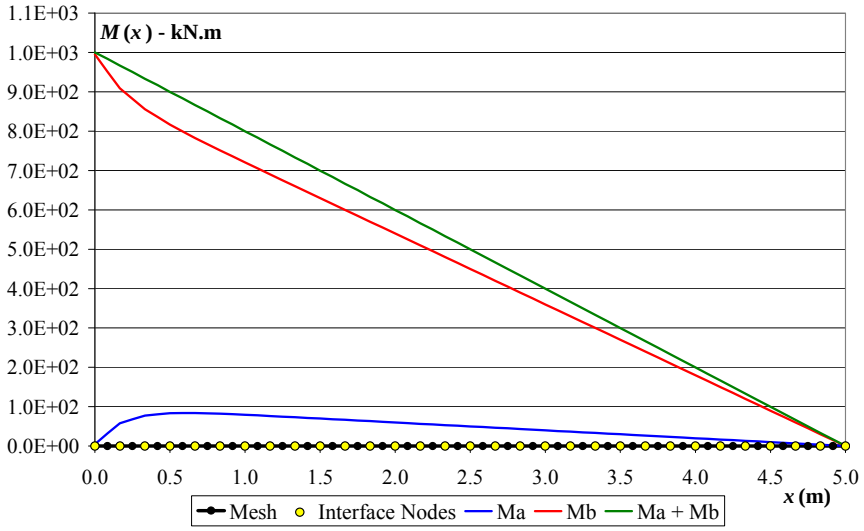

Figure 17: Bending moment distributions at each material section (*k = 1000*).

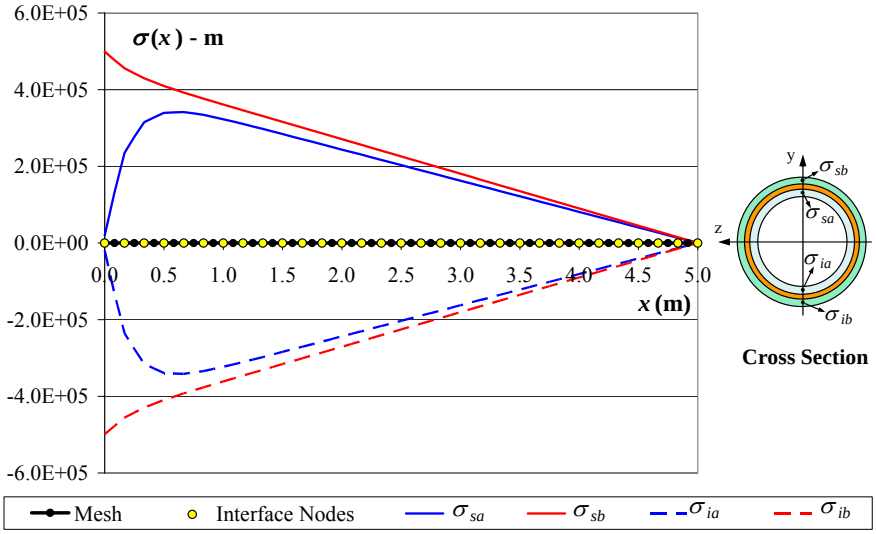

Figure 18: Axial stresses at each material layer (*k = 1000*).

4. CONCLUSIONS

This work has been focused on representing the behavior of layered straight beams, under general loading. Interface conditions are numerically represented as an "extra" layer under the assumption of constant shear deformations through the thickness, assumed small as compared to other cross section dimensions. An analytical solution is presented for a two layer pipe under axial loadings for the clamp-free condition. The result has been evaluated with the numerical model solutions and very good agreement was obtained. However, no simple solution was possibly obtained in considering other bending or torsion loading conditions; these solutions could only be assessed using the numerical model results.

The finite element formulation presents a combination of beam and interface elements, providing a simple yet robust and reliable tool for multilayered piping analyses, as shown in the solution results. Sensitive studies for the value of interface stiffness were also considered, granting the numerical model a reliable physical representation of the problem and providing it a good numerical platform to include, a next step, stick-slip friction conditions between layers.

5. ACKNOWLEDGEMENTS

The first author thanks the financial support provided by PUC-Rio and Petrobras during his doctoral studies.

6. REFERENCES

Bathe,K.J., Finite Element Procedures, Prentice-Hall. 1996.

Chen WQ, Wu Y-F, Xu RQ, State space formulation for composite beam-columns with partial interaction. Composites Science and Technology 67(11-12) (2007) 2500-2512.

Newmark NM, Siess CP, Viest IM, Tests and analysis of composite beams with incomplete interactions. Proc. Soc Exp Stress Anal, 9(1) (1951) 75-92.

Girhammar UA, Gopu VKA, Analysis of P-A effect in composite concrete/timber beam-columns. Proc. Of the Instit. Of Civil Engineers – Research and Theory, 91 (1991) 39-54.

Girhammar UA, Gopu VKA, Composite beam-columns with interlayer slip – exact analysis. ASCE J. of Structural Enging. 119(4) (1993) 1265-1282.

Girhammar UA, Pan D, Exact static analysis of partially composite beams and beam-columns. Int. J. of Mechanical Sciences 49 (2007) 239-255.

Girhammar UA, Composite beam-columns with interlayer slip – approximated analysis Int. J. of Mechanical Sciences 50 (2008) 1636-1649.

Jeong Y-J, Kim H-Y, Kim S-H Partial-interaction analysis with push-out tests, J. of Constr. Steel Research 61 (2005) 1318-1331.

Sousa Jr. JBM, Silva AR, Analytical and numerical analysis of multilayered beams with interlayer slip, Engineering Structures 32 (2010) 1671-1680.

Wu, Y-F, Xu R, Chen W, Free vibrations of the partial-interaction composite members with axial force. J. of Sound and Vibration 299 (2007) 1074-1093.

Xu R, Wu R, Chen W, Static, dynamic and buckling analysis of partial interaction composite members using Timoshenko's beam theory. Int. J. of Mechanical Sciences 49 (2007) 1139-1155.

Zona A, Ranzi, G, Finite element models for nonlinear analysis of steel-concrete composite beams with partial interaction in combined bending and shear, Finite Elements in Analysis and Design, 47 (2011) 98-118.

7. RESPONSIBILITY NOTICE

The authors are the only responsible for the printed material included in this paper.